Air Distribution in Rooms, (ROOMVENT 2000)
Editor: H.B. Awbi

STUDY ON VENTILATION PERFORMANCE AND INDOOR AIR QUALITY OF A PORTABLE CLASSROOM: FIELD MEASUREMENT AND NUMERICAL SIMULATION

J. Zeng, C. Y. Shaw, R. J. Magee, and D. Sander

Institute for Research in Construction, National Research Council
Canada, Ottawa, Ontario K1A 0R6, Canada

ABSTRACT

This paper describes an investigation into the ventilation performance and the indoor air quality of a portable classroom. Both field measurements and numerical simulations based on CFD (Computational Fluid Dynamics) technology were used. Field measurements in an unoccupied classroom used smoke to visualize the flow pattern, and hot-film probes to quantitatively measure air velocity. These field measurements provided the boundary conditions for CFD simulations and the experimental data to examine the accuracy of the CFD simulations. A CFD simulation of the unoccupied classroom showed good agreement with the field measurements. Additional CFD simulations were then conducted to predict the flow patterns and the distributions of the age of air and CO_2 concentration that would occur in the occupied classroom. The results indicated that the air environment in the portable classroom needed to be improved.

KEYWORDS

Portable classroom, Ventilation performance, Indoor air quality, Field measurement, and CFD

INTRODUCTION

Portable classrooms are widely used in Canada, because of their low-cost and mobility. Heating and ventilation (and sometimes cooling) for the portable classroom is usually provided by a simple ventilator unit. There is some concern about the ability of such ventilator units to provide good IAQ for students in portable classrooms [Thompson 1998]. The occupants produce CO_2 and contaminants such as odors (bio-effluents) [Wheeler 1998]. This creates a region around the occupants with relatively high local contaminant concentrations. School boards are interested in developing efficient and cost-effective ventilation systems for these classrooms.

This study incorporates both field measurements and computer simulation based on computational fluid dynamics (CFD). The benefits of the CFD approach have become recognized by researchers in the field of ventilation [Murakami et al. 1997; Chen 1997]. The field measurements provide information to establish boundary conditions for the CFD simulations and to determine the accuracy of simulation results.

CLASSROOM

Figure 1 illustrates the interior layout of the portable classroom that was investigated. It is 9.4m long × 6.9m wide × 2.4m high and accommodates 24 students in Grades 3 and 4 plus a teacher. The room contains 24 student desks and chairs, some tables, bookcases, cabinets, and a closet. For the CFD simulations, each student and his/her chair were represented by individual rectangular block with the dimensions of 0.3m × 0.2m × 0.8m, while the teacher with the dimensions of 0.45m × 0.45m × 1.7m.

Photo 1 shows the installed ventilator unit. It has a single high-mount supply air opening and a single low-mount return air opening. It is located close to the middle of the long wall between the two windows. The supply air opening is equipped with adjustable louvers to control the direction of supply air. The outdoor air is directly ducted to the ventilator unit. The supply air is composed of the outdoor air and the returned room air.

FIELD MEASUREMENTS

The field measurements were conducted during the summer vacation when the classroom was vacant. Thus, the classroom temperature, supply air temperature and outdoor temperature were all about 25°C. The tests, which consisted of visualizing airflow patterns and measurement of airflow rates and air velocities, are described below.

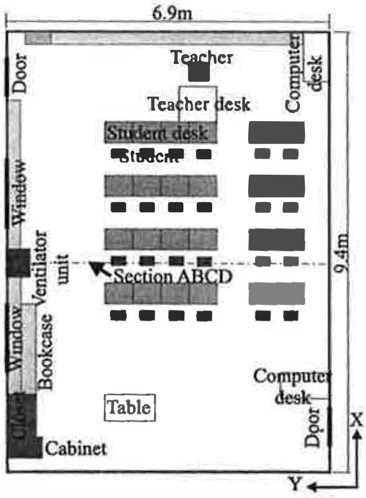

Figure 1: Layout of the classroom

Photo 1: Ventilator unit

Visualization Two types of smoke source, mosquito coil and smoke bomb, were used to visualize the airflow patterns. To identify the direction of the supply airflow and the airflow pattern within the classroom space, smoke from a smoke bomb was injected into the fresh air opening. The smoke then appeared in the supply air that was discharged to the classroom from the supply opening. Mosquito coils were used to visualize the local air movement in the Section ABCD, i.e., the central section of the ventilator unit.

Airflow rates A hood-type flow meter was used to measure the flow rate of fresh air, supply air and return air at the ventilator unit.

Air velocity Supply air velocity was measured with a portable velocimeter. Hot-film probes were used to measure the air velocity in the Section ABCD (cf. Figures 1). Both instruments were calibrated with a bench top wind tunnel prior to the measurements. 24 probes were set up on 4 stands to measure 4 profiles, as shown in Figure 3.

CFD SIMULATIONS

Two simulation cases were performed. Case 1 is a model of the unoccupied classroom at the same conditions as those under which the field measurements were taken. The purpose of this case is to check the accuracy of the CFD simulations. Case 2 is a model of the occupied classroom to investigate the air quality that would occur in this classroom.

The standard k-ε model [Launder and Spalding 1974] was used to predict the airflow in the classroom. The ventilation performance (age of air) [Murakami 1992] and air quality (CO_2 concentration) were calculated based on the predicted flowfield.

BOUNDARY CONDITIONS FOR CFD SIMULATIONS

Table 1 lists the boundary and other simulation conditions. The boundary conditions for supply velocity were determined from the measured supply airflow rate, the scalar supply velocity, the visualized supply airflow pattern and the observed direction of the supply louvers. Figure 2 illustrates the boundary conditions for the supply opening used in this paper. The supply air opening was modeled as three sub-areas 1, 2, and 3. The central sub-area 2 discharges supply air normal to the surface. The supply air from the two side sub-areas 1 and 3 had both the normal and the parallel velocity. In general, the supply air from the entire opening flows slightly downward to the floor (approximately 10°).

MEASURED AND SIMULATED FLOWFIELD IN UNOCCUPIED CLASSROOM - CASE 1

Airflow pattern Figure 3 shows the airflow pattern in the Section ABCD that was visualized by using smoke from mosquito coils. Figure 4(1) illustrates the predicted flowfield for the same section. There is good agreement between the measurements and the simulation results. The supply air flows from the ventilator unit on a downward path across the room finally impinging on the floor near the opposite wall. It then travels up the wall and back to the ventilator unit along the ceiling.

Figure 4(2) shows the predicted flow pattern in plan view at an elevation of 1m (breathing level for seated students). This view shows the supply air splitting at the opposite wall and traveling along the wall toward the corners, where it forms a swirling pattern toward the center of the room. Eventually, the air flows back toward the ventilator unit where it enters the low level return air opening. The flow pattern appears to be well mixed.

Velocity profiles Figure 5 shows the scalar velocity profiles at four locations in the Section ABCD (a-a: 0.5 m from the ventilator unit, b-b: 2.0 m; c-c: 3.5 m; d-d: 5.0 m, cf. Figure 3). The height at which the maximum velocity occurs for these four locations becomes lower with increasing distance from the ventilator unit. This is consistent with the downward flow path for supply air shown in figures 3 and 4. The maximum velocity of approximately 3.0m/s for

TABLE 1
BOUNDARY AND CALCULATION CONDITIONS

Supply	U_{in}, V_{in}, W_{in}: Figure 2 $k_{in}=3/2(0.05V_{in})^2$ $\varepsilon_{in}=C_\mu k_{in}^{3/2}/L_{in}$, $L_{in}=1/7\times$ width of supply CO_2: 612ppm
Return	Velocity, k, • , CO_2: free slip
Wall boundary	Standard log-law
grid	78 (x) × 51 (y) × 35 (z) = 139,230

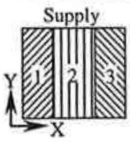

	Sub-area 1	Sub-area 2	Sub-area 3
U_{in} (m/s)	-4.5	0	4.5
V_{in} (m/s)	-2.1	-4.1	-2.1
W_{in} (m/s)	-0.8	-0.8	-0.8

Figure 2: Supply velocity

a-a occurs at a height of 1.7m, 1.1m/s for b-b at 1.3m, 0.7m/s for c-c at 0.5m. The air velocity in the occupied zone is significantly higher than the recommended minimum value (0.25m/s) [ASHRAE handbook fundamentals, 1997]. High air velocities may result in uncomfortable drafts and may even cause papers to be blown off desks.

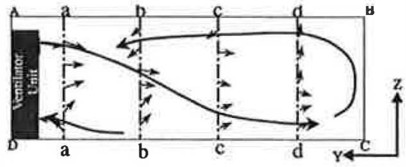

Figure 3: Visualized flow pattern

In general, the simulated scalar velocity agrees very well with the measured data. In a-a, the maximum velocity was not measured because of the probe location. Good agreement was obtained between the measurement and the simulation for both the values and the locations of the maximum velocities in b-b and c-c.

In d-d, there are some discrepancies between the measurement and the simulation. There are two possible reasons for these discrepancies. (1) The profile d-d is located at the region after the airflow impinging the floor (cf. Figures 3 and 4). The standard k-ε model has difficulty precisely predicting flow fields with impinging region, because of the overestimation of turbulence kinetic energy k in the impinging region [Kato and Launder 1993]. After the impinging region, the mean velocity is underestimated, as observed in d-d. (2) The velocity in d-d was generally lower than that in the other measured locations. Hot-film probes have lower precision in measuring low velocity [Chen and Glicksman 1998].

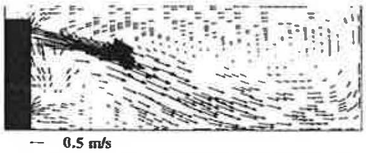

(1) Section ABCD (X=4.41m)

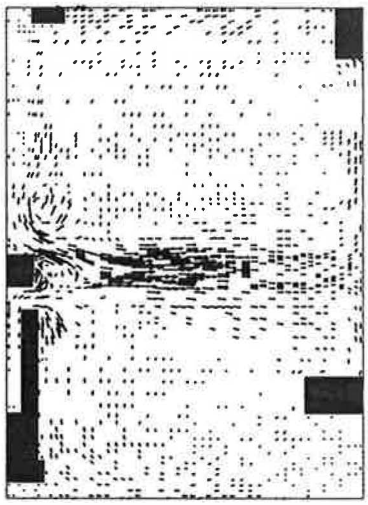
(2) Breathing level (Z=1.0m)

Figure 4: Predicted flow field

SIMULATED RESULTS IN OCCUPIED CLASSROOM - CASE 2

Characteristics of Flowfield

Figure 6 shows the simulated flowfield in the occupied classroom. Comparing to the scenario in the unoccupied classroom, this case has significantly lower velocity in the occupied zone due to the blocking effects of the

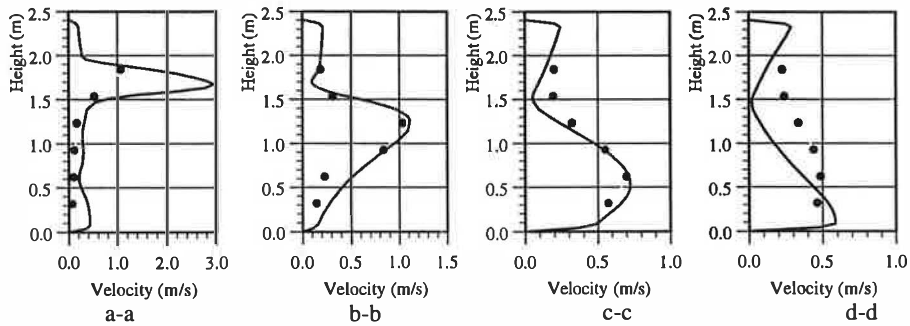

Figure 5: Profiles of scalar velocity in the Section ABCD
(Black circles: measured data, lines: CFD results)

occupants. However, several occupants close to the ventilator unit are still exposed to the high velocity, which causes uncomfortable draft. The flow patterns in plan view at the breathing level are similar to each other for both cases: unoccupied and occupied. The airflow is more active in the rear part than in the front part. The ventilator unit was located between the third row desks and the fourth ones, close to the middle line of the classroom. Thus, the classroom had more obstacles in the front part than in the rear part. These obstacles cause the blocking effects on the air movement.

Age of Air

Figure 7 shows the predicted age of air for both Section ABCD and in plan view at the breathing level. The age of air is an index to evaluate the ventilation performance [Sandberg 1992]. In Section ABCD, the air in the region near the supply opening was the youngest (freshest). The upper part of the space and lower part around the return had the age of air of 1.0. In the plan view at breathing level, the region directly in the path of the supply air had younger (fresher) air than the other regions. The age of air in the front part of the classroom was over 1.2, higher than that in the rear part of the classroom. This distribution property might be caused by the blocking effect of obstacles on the air movement.

The average age of air for the entire space, the occupied zone and the breathing level are 1.14, 1.14 and 1.16 respectively. The age of air for an ideal perfectly mixed flow field distributed uniformly through the entire space is 1.0. A smaller age of air indicates better ventilation efficiency in supplying the fresh air to that specified location.

CO_2 Concentration

The CO_2 concentration is a surrogate index to assess the air quality, especially for spaces with high occupant densities. The CO_2 generation rate is 20L/h per person [ASHRAE handbook fundamentals, 1997]. The outdoor CO_2 concentration is 350ppm. The simulation was performed based on the

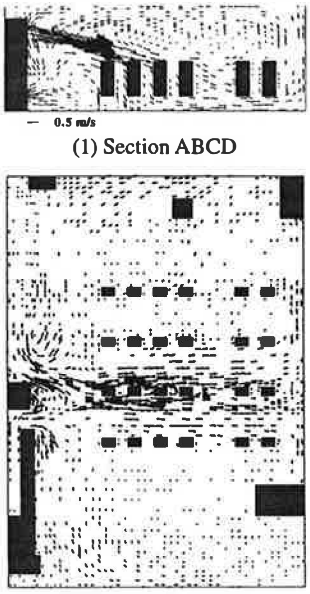

(1) Section ABCD

(2) Breathing level

Figure 6: Flowfield

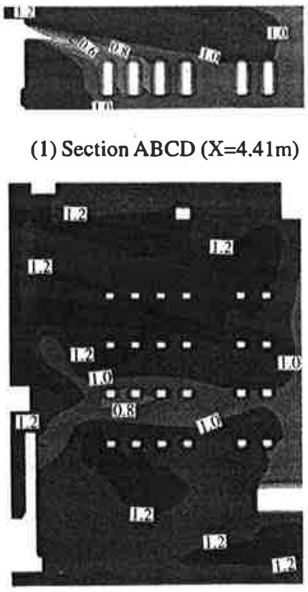

(1) Section ABCD (X=4.41m)

(2) Breathing level (Z=1.0m)

Figure 7: age of air

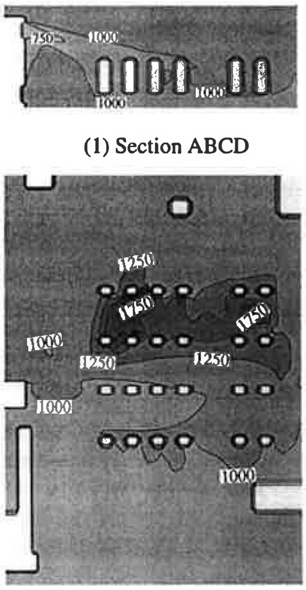

(1) Section ABCD

(2) Breathing level

Figure 8: CO_2 concentration

measured ratio of outdoor air to supply air (59%). The CO_2 concentration in the supply air was specified at 612ppm.

Figure 8 illustrates the predicted distribution of the CO_2 concentration. The front part of the classroom had higher CO_2 concentration than the rear part. This distribution characteristic might be explained by two reasons: (a) the front part had more CO_2 generation; (b) the ventilator unit provided less ventilation air to the front than to the rear (cf. Figure 7). Except for students close to the ventilator unit, most students and the teacher were exposed to an environment with CO_2 concentration higher than 1000ppm, which is the recommended maximum acceptable value [ASHRAE handbook fundamentals, 1997]. An optimized ventilator unit with more reasonable location of supply device may decrease the indoor CO_2 concentration. Further work needs to be done to check this feasibility.

CONCLUSIONS

Field measurements on a portable classroom provided experimental data for determining the boundary conditions and evaluating the accuracy of a CFD simulation. The measured data includes the visualized flow pattern, airflow rates, and velocity profiles through one section of the space.

Good agreement for airflow pattern and velocity were achieved between the measurements and the CFD simulation for the unoccupied classrooms.

A CFD simulation of the occupied classroom predicted the ventilation performance (age of air) and air quality (CO_2 concentration). The results indicate that draft might be experienced by some students. Furthermore, the occupants in the front part of the classroom would be exposed to higher CO_2 concentration than those in the rear part.

REFERENCES

ASHRAE handbook - fundamentals, (1997). Atlanta: American Society of Heating, Refrigerating and Air-conditioning Engineers, Inc.

Chen, Q., (1997). Computational fluid dynamics for HVAC: successes and failures. *ASHRAE Transactions*, **103:1**, 178-187.

Chen, Q.Y. and Glicksman, L. (1998). Performance evaluation and development of design guidelines for displacement ventilation. *ASHRAE Research Report*, **RP-949**.

Kato, M., Launder B.E. (1993). The modelling of turbulent flow around stationary and vibrating square cylinders. *Proceeding of 9th Symposium on Turbulent Shear Flows, Kyoto, Japan*, **10-4-1 – 10-4-6**.

Launder, B.E. and Spalding, D.B. (1974). The numerical computation of turbulent flows. *Computer Methods in Applied Mechanics and Energy*, **3**, 268-289.

Murakami, S. (1992). New scales for ventilation efficiency and their application based on numerical simulation of room airflow. *Proceedings of ISRACVE, University of Tokyo*, 22-37.

Murakami, S., Kato, S., and Zeng J., (1997). Flow and temperature fields around human body with various room air distribution, CFD study on computational thermal manikin (Part I). *ASHRAE Transactions*, **103:1**, 3-15.

Sandberg, M. (1992). Ventilation effectiveness and purging flow rate – a review. *Proceedings of ISRACVE, University of Tokyo*, 1-21.

Thompson, B. (1998). Engineers, IAQ, and schools. *ASHRAE Journal*, **June 1998**, 22-26.

Wheeler, A. E. (1998). System selection. *ASHRAE Journal*, **June 1998**, 12-16